Channel Model for Massive MIMO Shallow Underwater Acoustic Communications

Thomas Chové, Pierre-Jean Bouvet, Christophe Laot, Nicolas Le Josse

Channel Model for Massive MIMO Shallow Underwater Acoustic Communications

Thomas Chové*†‡, Pierre-Jean Bouvet†, Christophe Laot‡ and Nicolas le Josse*
* Thales, Brest, France
† ISEN Yncréa Ouest, Brest, France
‡ IMT Atlantique, Lab-STICC, UMR CNRS 6285, Brest, France

***Abstract*—Oceans are an environment attracting growing interest, with major economic stakes. There exists a need to design systems able to explore the underwater environment, one of the challenges being the ability to communicate undersea. The underwater acoustic channel is considered as being one of the most difficult environments for designing communication systems, due to multiple limitations (frequency band, latency, Doppler effect...).**

A method that could allow an increase of the data rate is the use of massive MIMO (multiple inputs, multiple outputs) systems, where many transducers are used to emit as well as to receive the signal. The objective of this paper is to present a model for a massive MIMO underwater acoustic communication channel in order to carry out a preliminary analysis of the impact of array correlation on the theoretical achievable rate by using Shannon capacity.

***Index Terms*—Underwater acoustic communication, Massive MIMO, Channel modeling**

I. Introduction

Underwater warfare tends to imply multi-platform systems, with more and more unmanned vehicles. Therefore, there is a need to design efficient underwater wireless communication systems, making possible control, monitoring and collaboration between heterogeneous platforms. The underwater channel is known to be one of the most challenging environments for communications. Optical and radio frequency communications are strongly limited, making acoustic waves the only viable solution for medium and long-range communications.

Underwater acoustic communications (UAC) come with several constraints. Even if spectrum regulations like those of terrestrial radio-frequency systems do not exist, the available frequency band is limited by the presence of noise at low frequencies and by absorption at high frequencies. Hardware limitations may also limit the frequency band. Multipath propagation in shallow water environment is also a source of inter-symbol interferences (ISI), and the low celerity of acoustic waves (1500 m/s, to be compared to the $3 \cdot 10^8$ m/s celerity of electromagnetic waves) leads to strong Doppler effect and latency. The underwater acoustic channel can then be qualified as strongly selective in time, frequency, and space.

The achievable effective data rate is often approximated as being inversely proportional to the distance between the transmitter and the receiver. For most commercial and academic systems, the range-data rate product is lower than 40 kbits $\cdot$ s^{-1} $\cdot$ km [1]; some academic studies have claimed results above 100 kbits $\cdot$ s^{-1} $\cdot$ km at ranges of the order of the kilometer in favorable conditions [2], [3], [4].

There is currently no consensus on a realistic channel model for underwater acoustic propagation. In some papers, deterministic ray-based models are used as an approximation, adding eventually random phase to each ray [5]. Random fluctuation path loss coefficients can also be generated based on statistical properties determined by the ray tracing model, in order to model the time selectivity of the channel [6]; the nature of the fluctuations can be chosen using entropy maximization, introducing no arbitrary knowledge of the channel [7]. Last, a hybrid method between experimentations and model-based simulations can be obtained using stochastic replay, where the channel is assumed to be the result of a random process of which a new realization can be generated [7], [8].

An interest concept to increase the so-called channel capacity [9], [10] and improve robustness against fading is massive MIMO, where one uses large numbers of transmit and receive elements (from a few tens to several hundreds [11]) such as the channel matrix's statistics (in particular the singular values distribution and thus the channel capacity) tend to be deterministic [11], [12], [13]. Such a technique is already being used for radio communications, *e.g.* with 5G [13]. Massive MIMO could also allow sparse channel estimation [5], [12]. However, massive MIMO might not be applicable to line of sight (LOS) point-to-point environments, for which the channel matrix is of limited rank [13], [14]. Another difficulty is channel estimation, as multiple channel impulse responses (CIR), fluctuating with time, are to be estimated [13]. Last, the transducers array cost and size may be a limitation to practical applications. To the best of the authors' knowledge, there is no multiple inputs, multiple outputs (MIMO) UAC channel model, taking into account the spatial correlation, in the existing literature.

In this paper, we propose a model for MIMO communication systems, which is presented in section II. A performance analysis, in which we study the effects of transducers correlation onto channel capacity, is proposed in section III. Finally, section IV gives the conclusion and perspectives of this work.

Notations

The below notations will be used in the following:

- $\mathbf{A}^H$ denotes the hermitian transpose of matrix $\mathbf{A}$;

- $\mathbb{E}(X)$ denotes the expectancy of the random variable X;
- $\mathbf{A}*\mathbf{B}$ denotes the convolution product of matrices $\mathbf{A}(t) \in \mathbb{C}^{K\times M}$ and $\mathbf{B}(t) \in \mathbb{C}^{M\times N}$, *i.e.*

$$\mathbf{A} * \mathbf{B}(t) = \int_{-\infty}^{+\infty} \mathbf{A}(\tau)\mathbf{B}(t-\tau)\mathrm{d}\tau \in \mathbb{C}^{K\times N};$$

- $\bullet$ is the input variable of a function, *e.g.* $f(\bullet, t)$ denotes the function $\tau \mapsto f(\tau, t)$ (with t a fixed variable);
- $\otimes$ denotes the Kronecker matrix product;
- $\mathcal{CN}(\mathbf{m}, \mathbf{V})$ denotes the circularly-symmetric multidimensional complex normal distribution, with expectancy $\mathbf{m} \in \mathbb{C}^N$ and covariance matrix $\mathbf{V} \in \mathbb{C}^{N\times N}$ ($N \in \mathbb{N}^*$ being the dimension).

II. Channel model

Our model is an extension to MIMO systems of the entropy-based channel proposed by [7]. Modeling a MIMO channel requires, in addition to the single input, single output (SISO) model, the modeling of spatial correlations between array elements.

Here, we assume a Kronecker structure for the correlation of diffuse components, as proposed by [15], [16], where the transmit and receive correlation arrays have the structure proposed by [16].

We consider here a MIMO system with N_t transducers at the transmitter and N_r hydrophones at the receiver. The base-band time-variant CIR is then modeled as $\mathbf{H}(\tau, t) \in \mathbb{C}^{N_r\times N_t}$. The input-output relationship is then given by

$$\mathbf{y}(t) = (\mathbf{H}(\bullet, t) * \mathbf{x})(t) + \mathbf{w}(t) \tag{1}$$

where $\mathbf{x}(t) \in \mathbb{C}^{N_t}$ is the input signal, $\mathbf{y}(t) \in \mathbb{C}^{N_r}$ is the output signal, $\mathbf{w}(t) \in \mathbb{C}^{N_r}$ is an additive noise.

The CIR is assumed to be the sum of L paths, whose delays and mean power are obtained by ray tracing, for instance, using the algorithm Bellhop [17], [18]. An example of ray tracing result obtained with Bellhop, showing the multipath propagation, is provided in figure 1. Each path has a different attenuation, depending on propagation (absorption, geometrical propagation losses) and reflection losses:

$$h_{n,m}(\tau, t) = \sum_{\ell=1}^{L} h_{n,m}^{(\ell)}(t)\delta(\tau - \tau_{n,m}^{(\ell)}(t)) \tag{2}$$

with $h_{n,m}^{(\ell)}(t)$ the complex attenuation from transducer m to hydrophone n on the ℓ^{th} path and $\tau_{n,m}^{(\ell)}(t)$ the associated delay. Each path's attenuation is decomposed as $h_{n,m}^{(\ell)}(t) = d_{n,m}^{(\ell)} + \tilde{h}_{n,m}^{(\ell)}(t)$ where $d_{n,m}(\ell)$ is a specular (deterministic) component and $\tilde{h}_{n,m}^{(\ell)}(t)$ is a diffuse (random) component [7] with

$$\tilde{h}_{n,m}^{(\ell)}(t) \sim \mathcal{CN}(0, \sigma_\ell^2).$$

The mean power p_ℓ of each path obtained by ray tracing yields $\left|d_{n,m}^{(\ell)}\right|^2 + \sigma_\ell^2 = p_\ell$ (we assume p_ℓ and σ_ℓ to be the same for all the transmitter-receiver pairs, for a given path); the Rice factor $K_\ell = \frac{\left|d_{n,m}^{(l)}\right|^2}{\sigma_\ell^2}$ is assumed here to be deterministic, decreasing exponentially with delay [7].

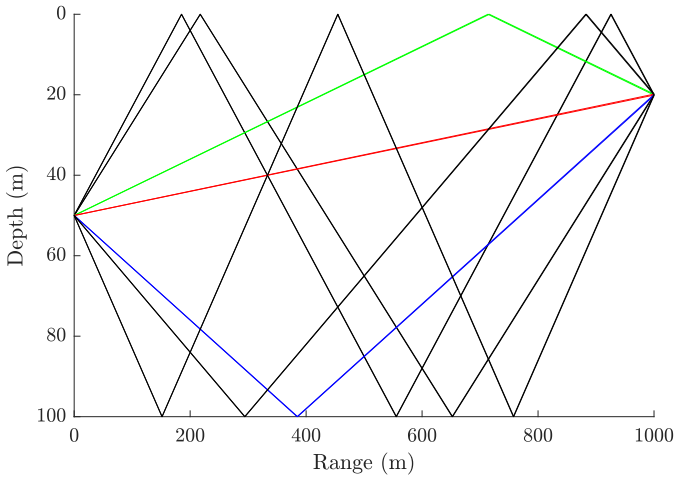

Fig. 1. Eigenrays plot obtained with Bellhop [17], for an isocelerity environment with 100 m depth, 1 km range (not to scale), with transmitter at 50 m depth and receiver at 20 m depth. Only rays with angle of departure between -20° and 20° are represented.

In order to define consistently the signal-to-noise ratio (SNR), we normalize here the CIR by

$$\sum_{\ell=1}^{L} p_\ell = 1 \tag{3}$$

We also normalize the noise to unit power, uniformly distributed over the frequency band: assuming that there is no privileged arrival direction for it, $\mathbf{w}$ has independent and identically distributed (i.i.d.) entries. Noise will then be modeled as being white, gaussian and uncorrelated: $\mathbf{w}(t) \sim \mathcal{CN}(\mathbf{0}, \mathbf{I})$. The CIR and noise being normalized, the SNR ρ is equal to the emitted power:

$$\rho = \mathbb{E}(\mathbf{x}^H(t)\mathbf{x}(t)). \tag{4}$$

One may note that array gain can be obtained thanks to processing techniques such as *beamforming*, and that the SNR of the processed signal might be higher than the one defined above; however, the definition above will be used in order to allow consistent comparison with SISO systems, for a same transmitted power.

Assuming that the diffuse component follows the "Kronecker correlation" assumption presented by [15], one may write

$$\mathbb{E}\left(\tilde{\mathbf{h}}_{\text{vec}}^{(\ell)}(t)\tilde{\mathbf{h}}_{\text{vec}}^{(\ell)H}(t)\right) = \sigma_\ell^2 \mathbf{\Psi}_r \otimes \mathbf{\Psi}_t \tag{5}$$

[15], [16], where $\tilde{\mathbf{h}}_{\text{vec}}^{(\ell)}(t)$ is a N_rN_t-elements column vector whose coefficients are $\tilde{h}_{n,m}^{(\ell)}(t)$ (stacked column by column as in [16]). The receive and transmit correlation matrices are denoted by $\mathbf{\Psi}_r \in \mathbb{C}^{N_r\times N_r}$ and $\mathbf{\Psi}_t \in \mathbb{C}^{N_t\times N_t}$ and are supposed to have structure $[\mathbf{\Psi}_{r,t}]_{i,j} = \psi_{r,t}^{|i-j|}$, where $|\psi_{r,t}| \in [0, 1]$ [16], this coefficient depending on the environment and of the arrays elements spacing.

The fluctuations of the $\tilde{h}_{n,m}^{(\ell)}(t)$ coefficients are modeled by their Doppler spectrum [7]:

$$S_{n,m}^{(\ell)}(\nu) = \int_{-\infty}^{+\infty} \mathbb{E}\left[\tilde{h}_{n,m}^{(\ell)}(t)\tilde{h}_{n,m}^{(\ell)*}(t+\xi)\right] e^{-2j\pi\nu\xi} \mathrm{d}\xi \quad (6)$$

whose entropy is maximized under the constraint of the first (zero-mean) and second (Doppler spread) moments [7].

III. Performance prediction

A. Capacity and bandwidth

Assuming the transmitter has no knowledge of the CIR, an upper bound on the achievable data rate can be estimated using Shannon second theorem [10]:

$$C(\nu,t) = \log_2 \det\left(\mathbf{I} + \rho \mathbf{H}_F(\nu,t)\mathbf{H}_F^H(\nu,t)\right) \quad (7)$$

where $C(\nu,t)$ is the capacity per unit of used frequency band (in bits$\cdot$s$^{-1}\cdot$Hz^{-1}) and $\mathbf{H}_F(\nu,t) = \mathcal{F}_\tau[\mathbf{H}](\nu,t)$ is the channel time-variant frequency response ($\mathcal{F}_\tau$ denoting the Fourier transform over delays). One may keep in mind that C is an upper bound, under several unrealistic assumptions (perfect channel knowledge at the receiver, gaussian distribution of the transmitted signal...): one may refer to [19] for more realistic bounds.

The capacity will be averaged over a frequency-band around the optimal frequency proposed by [20]: the predicted performances will be given as

$$\bar{C} = \frac{1}{B}\int_{f_c-\frac{B}{2}}^{f_c+\frac{B}{2}} C(\nu)\mathrm{d}\nu, \quad (8)$$

where B is the bandwidth and f_c the center frequency. This frequency band is defined using well-known models of attenuation and noise, giving the optimal frequency described in [20] and given in figure 2. The bandwidth will here be taken as $B = \frac{f_c}{10}$, in order to take into account a realistic bandwidth-over-carrier ratio regarding transducer performances. It is noteworthy that the available bandwidth decreases with distance. As the data rate can be expressed as a function of the spectral efficiency (which can be upper-bounded at a given SNR and array configuration) and of the bandwidth, this will have an adverse effect on the achievable rate.

B. Performances

A shallow water environment is simulated with 100 m depth. The transmit array is located at 50 m depth and the receive array at 20 m depth. Both arrays have 4 m aperture with respectively N_t and N_r elements: the distance between successive elements depends on N_t and N_r. All simulation parameters are summarized in table I; the environment geometry parameters are defined in figure 3. Two parameters are still arbitrary and will need further analysis: the correlation coefficient, linked to the spatial coherence radius, has been fixed to $\psi = 0.9$ – this yields a coherence radius

$$L_c = -\frac{D_{t,r}}{2(N_{t,r}-1)\ln\psi_{t,r}} = 0.6 \text{ m}, \quad (9)$$

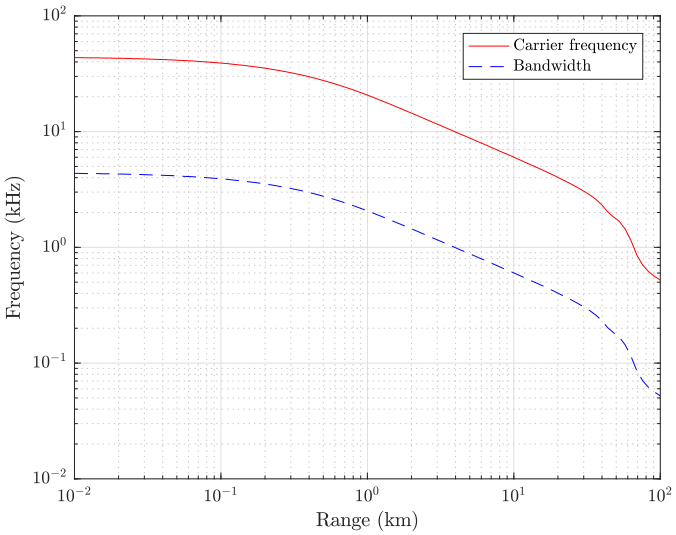

Fig. 2. Theoretical optimum center frequency (red plain line) – as defined in [20] – and bandwidth (blue dashed line) as a function of distance

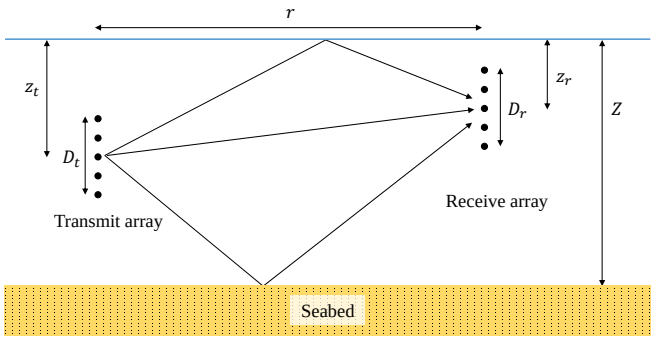

Fig. 3. Definition of the geometrical environment parameters

Symbol	Parameter	Value
Z	Water depth	100 m
z_t	Transmitter depth	50 m
z_r	Receiver depth	20 m
N_t	Transmit elements number	33
N_r	Receive elements number	33
$\psi_{t,r}$	Successive elements correlation	0.9
$D_{t,r}$	Transmit/receive array aperture	4 m
r	Range	100 – 5000 m
c_0	Sound speed in water	1500 m/s
ρ_0	Water density	1.0 kg $\cdot$ m^{-3}
c_{sb}	Sound speed in the seabed	1600 m/s
ρ_{sb}	Seabed density	1.8 kg $\cdot$ m^{-3}
K_{max}	First path's Rice factor	50
$t_{K,decay}$	Rice factor characteristic decay time	0.5 ms
$\nu_{dop,min}$	Minimum Doppler spread	0.5 Hz
$\nu_{dop,max}$	Maximum Doppler spread	2 Hz
ρ	Signal-to-Noise Ratio (SNR)	20 dB

TABLE I
Environmental parameters used for simulation

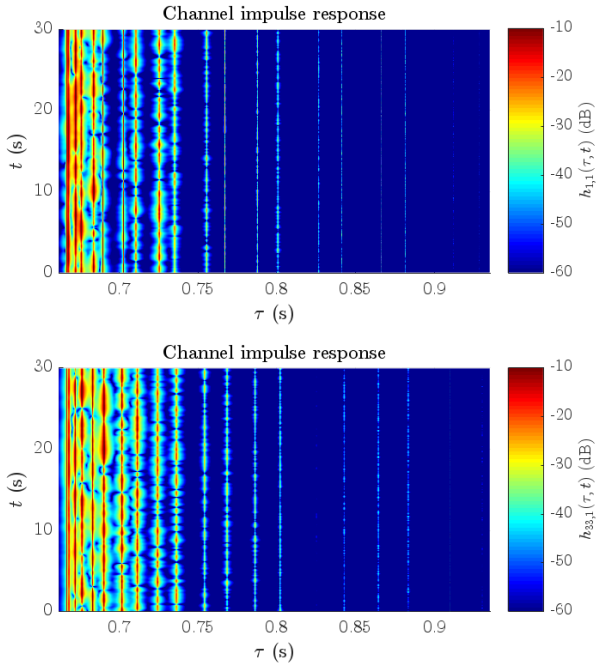

(a)

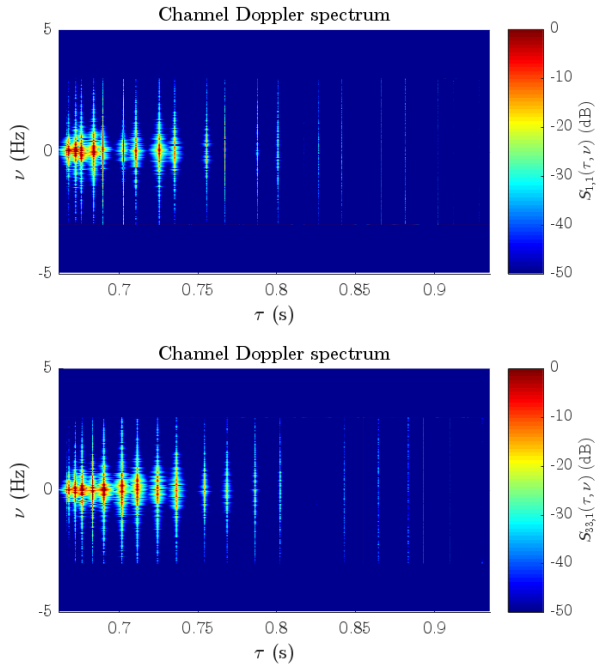

(b)

Fig. 4. (a) Time-variant channel impulse response and (b) associated Doppler spectrum, between transmitter #1 and receivers #1 and #33, with 1 km range, on 2 kHz bandwidth with carrier frequency $f_c = 15$ kHz

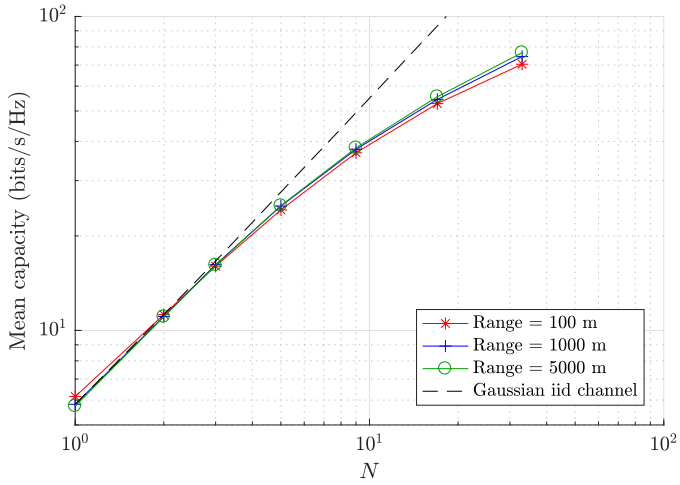

Fig. 5. Channel capacity for $\rho = 20$ dB with perfect channel knowledge at the receiver, averaged over the frequency band, as a function of transmit and receive elements number, and capacity of the gaussian i.i.d. channel

consistently with the order of magnitude that have been observed in the ALMA2017 experiment [21].

A sample of time-variant CIR, with the associated Doppler spectrum, between one source transducer and two different hydrophones, is given in figure 4. It is noteworthy that, even if the general structure of the responses are similar, the responses of the different hydrophones present weakly correlated fading. One may note that, given that no motion was introduced and that path delays are assumed deterministic, no change can be observed on path delays.

The channel is simulated for different ranges (from 100 m to 5 km), using 20 realizations for each range; for each realization, 1 s of time-variant CIR is generated with sampling frequency 10 Hz in the time domain and 30 kHz in the delay domain, yielding a total number of 200 CIRs realizations for each range. To determine the effect of MIMO arrays, the performance is calculated using only some elements of both transmit and receive arrays, from the SISO (1×1) to the 33×33 MIMO case; except for the SISO case, all simulated arrays are equally-spaced with 4 m aperture (*e.g.* the 5×5 array is simulated using elements $\#\{1, 9, 17, 25, 33\}$ of the 33×33 array).

In figure 5, the capacity, averaged over the frequency band, is given for different ranges (100 m in red stars, 1 km in blue crosses, 5 km in green circles) as a function of the arrays elements number. The performances of the modeled channel are compared to the ones of the ideal gaussian i.i.d. channel proposed by [10], representing the full diversity case. We assume here a constant SNR (set to $\rho = 20$ dB), which implies a greater emitted power for a greater range.

For a constant SNR, the channel capacity (in bits/s/Hz) has weak dependency with the range; this will not be the case for the data rate, which also depends on the available frequency band and is therefore a decreasing function of the range [20].

One may note that the channel capacity increases proportionally with $N = N_t = N_r$ when N is low, while it is not the

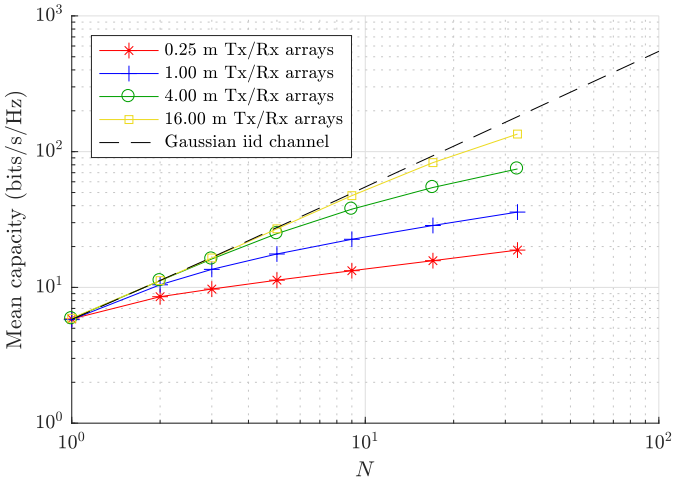

Fig. 6. Channel capacity for $\rho = 20$ dB with perfect channel knowledge at the receiver, averaged over the frequency band, as a function of transmit and receive element number, for different array apertures with constant coherence length, at 1 km range

case for large arrays, having low elements spacing and strong spatial correlation, that does not achieve the full diversity.

C. Effects of array correlation

In order to study the effects of the lack of diversity of correlated arrays on the achievable rate, the channel capacity was predicted for different array apertures. The correlation coefficient ψ was scaled in order to maintain a constant spatial coherence radius, *i.e.* it was taken as $\psi = 0.9^{D/D_{\text{ref}}}$ where $D_{\text{ref}} = 4$ m.

The predicted channel capacity at 1 km range is given in figure 6, for $D_t = D_r = 0.25$ m (red stars), $D_t = D_r = 1$ m (blue crosses), $D_t = D_r = 4$ m (green circles) and $D_t = D_r = 16$ m (yellow squares). It is noteworthy that, when the number of transducers increases with a constant array aperture, the full diversity capacity is achieved until the distance between to neighboring transducers is less or of the order of the coherence radius (recalling that $L_c = 0.6$ m, this transducers number limit is reached for $N \approx 27$ for a 16 m array or $N \approx 7$ for a 4 m array). When this condition is not respected, a loss of capacity is observed: for example, with 33 transducers at each side, the capacity is 4 times lower with 1 m-aperture antennas than in the full diversity case.

IV. Conclusion

In this paper, a MIMO extension of an existing channel model has been constructed, using a simple correlation structure, and was used in order to give a qualitative analysis of the effects of correlation onto the achievable spectral efficiency for underwater acoustic communications.

It was shown that, if the capacity of a widely-spaced arrays system may be proportional to the number of transducers at each side, this will not be the case when the distance between successive array elements is smaller or of the order of the spatial coherence radius. This will have to be taken into account when designing transducers arrays in order to find a balance between array size and elements correlation.

Several elements can be improved in the proposed model, in order to have experiment-based values for parameters such as the Rice factor and Doppler spread; more elaborated correlation structures are also to be investigated. An other aspect of MIMO that has not been taken into account here is the pilot overhead, which may increase with N_t. Accounting for these elements may lead to a realistic model that could be used in the first steps of the designing process of a communication system.

Acknowledgments

The authors thank Prof. François-Xavier Socheleau (IMT Atlantique, Lab-STICC) for his helpful comments and advices.

This work is supported by the French Department of Higher Education and Research under Grant No. CIFRE 2022/0971.

References

[1] M. Stojanovic and P.-P. J. Beaujean, "Acoustic communication," in *Springer Handbook of Ocean Engineering*, M. R. Dhanak and N. I. Xiros, Eds. Cham: Springer International Publishing, 2016, pp. 359–386. [Online]. Available: http://link.springer.com/10.1007/978-3-319-16649-0_15

[2] A. Tadayon and M. Stojanovic, "Low-complexity superresolution frequency offset estimation for high data rate acoustic OFDM systems," *IEEE Journal of Oceanic Engineering*, vol. 44, no. 4, pp. 932–942, Oct. 2019. [Online]. Available: https://ieeexplore.ieee.org/document/8488526/

[3] A. Rafati, H. Lou, and C. Xiao, "Soft-decision feedback turbo equalization for LDPC-coded MIMO underwater acoustic communications," *IEEE Journal of Oceanic Engineering*, vol. 39, no. 1, pp. 90–99, Jan. 2014. [Online]. Available: http://ieeexplore.ieee.org/document/6479709/

[4] P.-P. Beaujean and L. LeBlanc, "Spatio-temporal processing of coherent acoustic communications data in shallow water," in *OCEANS 2000 MTS/IEEE Conference and Exhibition. Conference Proceedings (Cat. No.00CH37158)*, vol. 3. Providence, RI, USA: IEEE, 2000, pp. 1625–1631. [Online]. Available: http://ieeexplore.ieee.org/document/882173/

[5] W. Wu, X. Gao, C. Sun, and G. Y. Li, "Shallow underwater acoustic massive MIMO communications," *IEEE Transactions on Signal Processing*, vol. 69, pp. 1124–1139, 2021. [Online]. Available: https://ieeexplore.ieee.org/document/9318541/

[6] P. Qarabaqi and M. Stojanovic, "Statistical characterization and computationally efficient modeling of a class of underwater acoustic communication channels," *IEEE Journal of Oceanic Engineering*, vol. 38, no. 4, pp. 701–717, Oct. 2013. [Online]. Available: http://ieeexplore.ieee.org/document/6616000/

[7] F.-X. Socheleau, C. Laot, and J.-M. Passerieux, "A maximum entropy framework for statistical modeling of underwater acoustic communication channels," in *OCEANS'10 IEEE SYDNEY*. Sydney, Australia: IEEE, May 2010, pp. 1–7. [Online]. Available: http://ieeexplore.ieee.org/document/5603811/

[8] P. van Walree, R. Otnes, and T. Jenserud, "Watermark: A realistic benchmark for underwater acoustic modems," in *2016 IEEE Third Underwater Communications and Networking Conference (UComms)*. Lerici, Italy: IEEE, Aug. 2016, pp. 1–4. [Online]. Available: http://ieeexplore.ieee.org/document/7583423/

[9] C. E. Shannon, "Communication in the presence of noise," *Proceedings of the IRE*, vol. 37, no. 1, pp. 10–21, Jan. 1949. [Online]. Available: http://ieeexplore.ieee.org/document/1697831/

[10] E. Telatar, "Capacity of multi-antenna gaussian channels," *European Transactions on Telecommunications*, vol. 10, no. 6, pp. 585–595, Nov. 1999. [Online]. Available: https://onlinelibrary.wiley.com/doi/10.1002/ett.4460100604

[11] F. Rusek, D. Persson, B. K. Lau, E. G. Larsson, T. L. Marzetta, and F. Tufvesson, "Scaling up MIMO: opportunities and challenges with very large arrays," *IEEE Signal Processing Magazine*, vol. 30, no. 1, pp. 40–60, Jan. 2013. [Online]. Available: http://ieeexplore.ieee.org/document/6375940/

[12] M. Wang, F. Gao, S. Jin, and H. Lin, "An overview of enhanced massive MIMO with array signal processing techniques," *IEEE Journal of Selected Topics in Signal Processing*, vol. 13, no. 5, pp. 886–901, Sep. 2019. [Online]. Available: https://ieeexplore.ieee.org/document/8794743/

[13] T. L. Marzetta, E. G. Larsson, H. Yang, and H. Q. Ngo, *Fundamentals of massive MIMO*, 1st ed. Cambridge University Press, Nov. 2016. [Online]. Available: https://www.cambridge.org/core/product/identifier/9781316799895/type/book

[14] L. Lu, G. Y. Li, A. L. Swindlehurst, A. Ashikhmin, and R. Zhang, "An overview of massive MIMO: benefits and challenges," *IEEE Journal of Selected Topics in Signal Processing*, vol. 8, no. 5, pp. 742–758, Oct. 2014. [Online]. Available: http://ieeexplore.ieee.org/document/6798744/

[15] C. Xiao, J. Wu, S.-Y. Leong, Y. R. Zheng, and K. B. Letaief, "A discrete-time model for triply selective MIMO Rayleigh fading channels," *IEEE Transactions on Wireless Communications*, vol. 3, no. 5, pp. 1678–1688, Sep. 2004. [Online]. Available: http://ieeexplore.ieee.org/document/1343903/

[16] J. Cross, J. Zhang, and Y. R. Zheng, "Impact of spatial correlation of fading channels on the performance of MIMO underwater communication systems," in *2011 - MILCOM 2011 Military Communications Conference*. Baltimore, MD, USA: IEEE, Nov. 2011, pp. 430–434. [Online]. Available: http://ieeexplore.ieee.org/document/6127707/

[17] M. B. Porter, "Acoustics toolbox," 2020. [Online]. Available: http://oalib.hlsresearch.com/AcousticsToolbox/

[18] M. B. Porter and Y.-C. Liu, "Finite-element ray tracing," in *Proceedings of the International Conference on Theoretical and Computational Acoustics*, vol. 2, 1994, pp. 947–956. [Online]. Available: https://hlsresearch.com/personnel/porter/papers/ICTCP%20ray%20paper.pdf

[19] P.-J. Bouvet and Y. Auffret, "On the achievable rate of multiple-input–multiple-output underwater acoustic communications," *IEEE Journal of Oceanic Engineering*, vol. 45, no. 3, pp. 1126–1137, Jul. 2020. [Online]. Available: https://ieeexplore.ieee.org/document/8737846/

[20] M. Stojanovic, "On the relationship between capacity and distance in an underwater acoustic communication channel," in *Proceedings of the 1st ACM international workshop on Underwater networks - WUWNet '06*. Los Angeles, CA, USA: ACM Press, 2006, p. 41. [Online]. Available: http://portal.acm.org/citation.cfm?doid=1161039.1161049

[21] G. Beaumont, A. Drémeau, R. Fablet, G. Real, and F. Le Courtois, "At-sea experimental evaluation of the influence of environmental fluctuations on the acoustic coherence radius," in *Underwater Acoustics Conference*, Heraklion, Greece, Jun. 2019. [Online]. Available: https://hal.science/hal-02330148